Journal of Membrane Science 321 (2008) 90–93

Contents lists available at ScienceDirect

Journal of Membrane Science

journal homepage: www.elsevier.com/locate/memsci

Nanocomposite membranes containing positively polarized gold nanoparticles for facilitated olefin transport

Sang Wook Kang[a], Jinkee Hong[a], Jong Hyuk Park[b], Sung Hyun Mun[c], Jong Hak Kim[d], Jinhan Cho[e], Kookheon Char[a], Yong Soo Kang[c,*]

[a] School of Chemical & Biological Engineering and NANO Systems Institute-National Core Research Center, Seoul National University, Seoul 151-744, South Korea
[b] Hybrid Materials Research Center, Korea Institute of Science & Technology, Seoul 136-791, South Korea
[c] Department of Chemical Engineering, Hanyang University, Seungdong-ku, Seoul 133-791, South Korea
[d] Department of Chemical Engineering, Yonsei University, Seoul 120-749, South Korea
[e] School of Advanced Materials Engineering, Kookmin University, Seoul 136-702, South Korea

ARTICLE INFO

Article history:
Received 17 April 2008
Accepted 18 April 2008
Available online 26 April 2008

Keywords:
Au nanoparticle
Membrane
Facilitated transport
Olefin

ABSTRACT

Positively polarized gold nanoparticles have been demonstrated for use as stable olefin carriers for facilitated olefin transport membranes. The formation and size of gold nanoparticles stabilized by 4-dimethylaminopyridine (DMAP) were monitored using X-ray diffraction (XRD), transmission electron microscopy (TEM) and UV–visible spectroscopy. Nanocomposite membranes that deliver high separation performance for olefin/paraffin mixtures were prepared by dispersing gold nanoparticles stabilized by DMAP in a polymer matrix, poly(vinyl pyrrolidone) (PVP). X-ray photoelectron spectroscopy (XPS) and zeta potential measurements revealed that gold nanoparticles stabilized by DMAP exhibited a high positive polarity, which is responsible for the reversible interaction between the gold nanoparticles and olefin molecules. Compared to neat PVP membranes, the composite membranes consisting of PVP and the polarized gold nanoparticles showed stable and enhanced separation of olefin/paraffin mixtures.

1. Introduction

Over the last decade, metal nanoparticles and nanocomposite have received increased attention due to their novel properties that are not often present on a larger scale [1–20]. The unique properties of nanomaterials result from their small size and large-specific surface area.

Among such materials, silver nanoparticles have attracted much interest due to their suitability for various applications, such as electronic conductors, catalysts, antimicrobials, and surface-enhanced Raman spectroscopy [1–5]. In particular, the polarized property of silver nanoparticles can be explained by the fact that the interaction of elemental O_2 with Ag nanoparticles of various sizes results in an increased capability of smaller nanoparticles to dissociate dioxygen to the atomic species, whereas the adsorbed oxygen species on bulk Ag at 80 K is predominantly O_2^- [21]. It has been recently reported that silver nanoparticles can be successfully utilized as an olefin carrier for facilitated olefin transport membranes [22]. Silver nanoparticles are partially polarized by an electron acceptor, such as *p*-benzoquinone, and thus reversibly interact with olefin molecules [22]. For example, a composite membrane consisting of poly(ethylene-co-propylene) (EPR), Ag nanoparticles, and *p*-benzoquinone at a 1:1:0.85 weight ratio has a propylene/propane selectivity of 11 and a total mixed gas permeance of 0.5 GPU (1 GPU = 1×10^{-6} cm^3 (STP)/(cm^2 s cmHg) [22].

In this work, the use of gold nanoparticles as an olefin carrier is investigated, making use of the fact that gold nanoparticles stabilized by 4-dimethylaminopyridine (DMAP) are expected to be highly polarized [8]. As far as we know, this is the first report of the successful use of positively polarized gold nanoparticles as a new olefin carrier for facilitated olefin transport membranes.

2. Experimental

2.1. Materials

Gold nanoparticles were prepared as reported previously [23]. Briefly, a 30-mM aqueous metal chloride solution ($HAuCl_4$, 30 mL) was added to a 25-mM solution of tetraoctylammonium bromide in toluene (80 mL). A 0.4-M solution of freshly prepared $NaBH_4$ (25 mL) was added to the stirred mixture, which caused an immediate reduction reaction to occur. After 30 min the two phases

* Corresponding author. Tel.: +82 2 2220 2336; fax: +82 2 2298 4101.
E-mail address: kangys@hanyang.ac.kr (Y.S. Kang).

0376-7388/$ – see front matter © 2008 Elsevier B.V. All rights reserved.
doi:10.1016/j.memsci.2008.04.047

were separated and the toluene phase was subsequently washed with 0.1 M H_2SO_4, followed by 0.1 M NaOH, and lastly H_2O, and then the toluene phase was dried over anhydrous $NaSO_4$, yielding the gold nanoparticles. An aqueous 0.1 M 4-dimethylaminopyridine solution (1 mL) was added to aliquots (1 mL) of the as-prepared nanoparticle mixtures. The 0.1 M concentration of the DMAP solution was found to be sufficient to cause complete and spontaneous phase transfer of the nanoparticles. Direct phase transfer across the organic/aqueous phase boundary was completed within 1 h, with no stirring or agitation. Solid DMAP was added directly to the toluene solution to precipitate the particles, which could then be resuspended in water [23]. Poly(vinyl pyrrolidone) (PVP) ($M_W = 1 \times 10^6$) was purchased from Aldrich Chemical Co. All of the chemicals were used as received.

2.2. Characterization

X-ray diffraction (XRD) with Cu Kα radiation was utilized at a scanning speed of 10°/min. Transmission electron microscopy (TEM) was performed using a Philips CM30 microscope operating at 300 kV. UV–vis absorption spectra were acquired using an OPTIZEN 2120UV. The IR measurements were performed on a Nicolet FT-IR spectrophotometer. For these measurements, 32 scans were signal-averaged at a resolution of 4 cm^{-1}. X-ray photoelectron spectroscopy (XPS) data were acquired using a PerkinElmer Physical Electronics PHI 5400 X-ray photoelectron spectrometer. This system was equipped with a Mg X-ray source operated at 300 W (15 kV, 20 mA). The carbon (C 1s) line at 285.0 eV was used as the reference in our determinations of the binding energies of the silver nanoparticles. The zeta potential of Au nanoparticles stabilized by DMAP in water was acquired using the OTSUKA ELS-8000.

2.3. Separation performance

The PVP/Au nanoparticle composite membranes were prepared by blending Au nanoparticles dispersed in water with PVP dissolved in ethanol. The [PVP]:[Au] weight ratio was fixed at 1:4.3, respectively. For fabrication of the separation membranes, the mixed solution was coated onto polysulfone microporous membrane supports (Seahan Industries Inc., Seoul, Korea) using an RK Control Coater (Model 101, RK Print-Coat Instruments Ltd., UK). After evaporation of the solvent in a convection oven at room temperature under nitrogen, the PVP/Au nanoparticle composite membranes were dried completely in a vacuum oven for 2 days at room temperature. The thickness of the top polymer electrolyte layer was found to be approximately 5 μm as determined by scanning electron microscopy (SEM). Gas flow rates and gas permeances were measured with a mass flow meter (MFM). The unit of gas permeance is GPU, where 1 GPU = 1×10^{-6} cm^3 (STP)/(cm^2 s cmHg). The mixed gas (50/50%, v/v propylene/propane mixture) separation properties of the PVP/Au nanoparticle composite membranes were evaluated using a gas chromatograph (Hewlett-Packard G1530A) equipped with a thermal conductivity detector (TCD) and a unibead 2S 60/80 packed column.

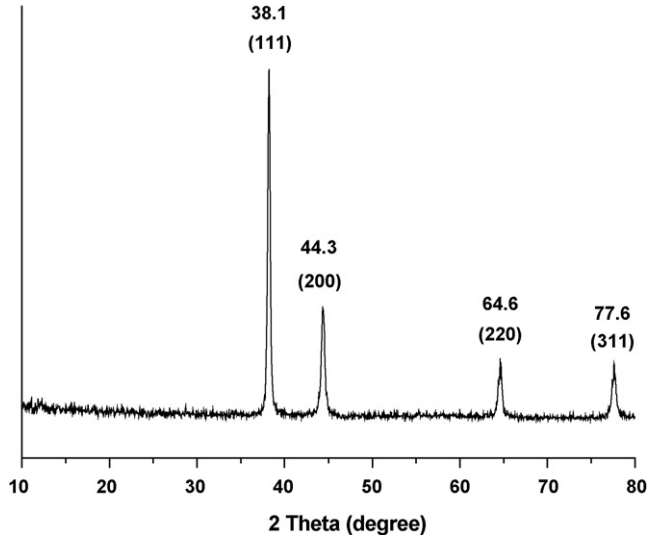

Fig. 1. XRD spectrum of the Au nanoparticles.

3. Results and discussions

3.1. Formation of gold nanoparticles

Gold nanoparticles were prepared from a $HAuCl_4$ solution in toluene with a reducing agent, $NaBH_4$, and a stabilizer, DMAP. XRD spectra were obtained to confirm the formation of gold nanoparticles. Fig. 1 shows the XRD patterns of gold nanoparticles stabilized by DMAP. The Au nanocomposites exhibited several prominent

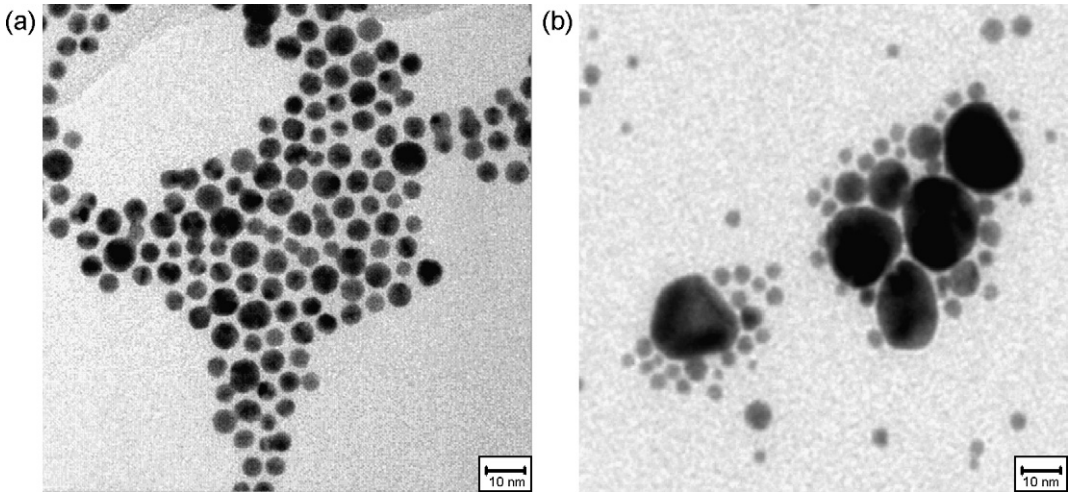

Fig. 2. TEM images of (a) Au nanoparticles stabilized by DMAP and (b) Au nanoparticles without DMAP.

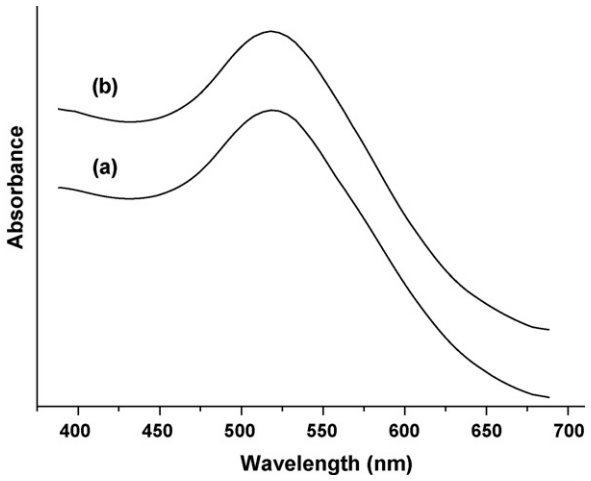

Fig. 3. UV–vis spectra of (a) Au nanoparticles stabilized by DMAP and (b) DMAP-stabilized Au nanoparticle/PVP composite.

peaks at 2θ values of about 38.1°, 44.3°, 64.6°, and 77.6° attributable to the (1 1 1), (2 0 0), (2 2 0), and (3 1 1) Bragg's reflections of the face-centered cubic structure of gold, respectively [24].

The formation and size of gold nanoparticles stabilized by DMAP were monitored using TEM. TEM images of the samples, shown in Fig. 2(a), clearly indicates that the average size of the gold nanoparticles stabilized by DMAP was about 5.5 nm and the particles had a uniform distribution of sizes. On the other hand, for the case of gold nanoparticles without DMAP, most of the particles aggregated, as shown in Fig. 2(b).

UV–vis absorption spectra are known to be quite sensitive to the formation of gold nanoparticles [23]. Fig. 3 presents the UV–vis absorption spectra for gold nanoparticles stabilized by DMAP and composite films containing PVP/Au nanoparticles stabilized by DMAP. One strong absorption peak was observed, centered at 518 nm for the two samples and corresponding to the plasmon excitation of gold nanoparticles. It is generally accepted that an absorption peak with a maximum occurring at around 518 nm is related to the formation of gold metal nanoparticles [23]. It is also known that the height of the peak provides information on the concentration of gold nanoparticles, and the peak position indicates the size of the gold nanoparticles. The full-width at half maximum (FWHM) may also be related to the size distribution of the nanoparticles. The symmetric UV–vis spectra indicate that the prepared gold nanoparticles were uniformly distributed. Furthermore, the peak shape did not change even when PVP was incorporated with the gold nanoparticles. Therefore, this UV–vis spectroscopic data demonstrates that the gold nanoparticles prepared in our work have a small size and a narrow distribution of size, which is consistent with the information obtained from the TEM images in Fig. 2.

3.2. Polarity of gold nanoparticles

The Au $4f_{7/2}$ regions of the XPS spectra for gold nanocomposite films are indicative of the chemical environment surrounding the gold and can provide important information for confirming the surface charge of the gold metal [10]. The binding energy of the $4f_{7/2}$ orbital of the gold nanoparticles stabilized by DMAP was 84.65 eV, while that for the case of gold nanoparticles without DMAP was 83.31 eV, as shown in Fig. 4. The value of 84.65 eV for the DMAP-stabilized gold nanoparticles was higher than the 83.5 eV (average size = 1.3 nm) reported in other research [25]. The higher value is presumably due to the fact that the surface of the gold nanoparticles was modified by DMAP and thus partially positively polarized.

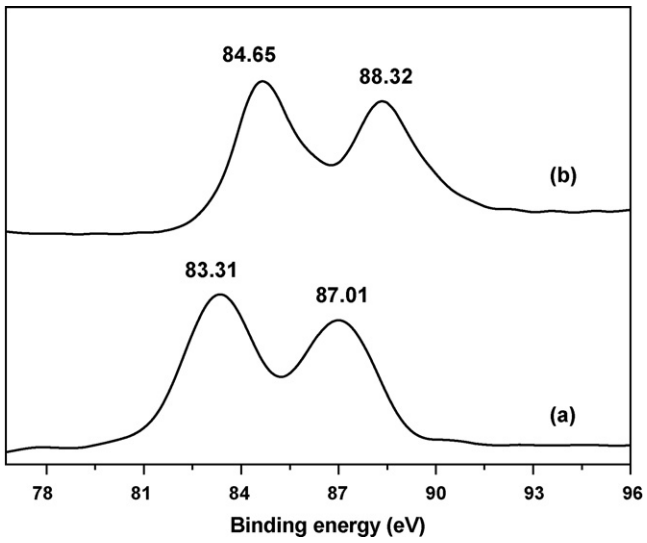

Fig. 4. Binding energy of (a) Au nanoparticles without DMAP and (b) Au nanoparticles stabilized by DMAP.

Table 1
Zeta potentials of Au nanoparticles

	Zeta potential (mV)
Au nanoparticles stabilized by DMAP	49.97
Au nanoparticles without DMAP	5.34

The measured zeta potentials also support this interpretation. The zeta potential of gold nanoparticles stabilized by DMAP was measured to be 49.97 mV, while that for the case of gold nanoparticles without DMAP was 5.34 mV; the zeta potentials are listed in Table 1. The higher value for the zeta potential of the gold nanoparticles with DMAP is presumably attributed to the partially positive polarized surface of the gold nanoparticles due to DMAP, which is consistent with XPS.

Therefore, the prepared gold nanoparticles are expected to have a partial positive charge on the surface, with which olefins may interact. If such an interaction is available, the positively charged nanoparticles may act as an olefin carrier for facilitated olefin transport.

To identify the potential interaction between PVP and the gold nanoparticles, FT-IR spectroscopy was utilized. The FT-IR spectra in Fig. 5 shows that the free carbonyl oxygen of neat PVP was observed at 1670 cm^{-1}. When the gold nanoparticles were introduced into

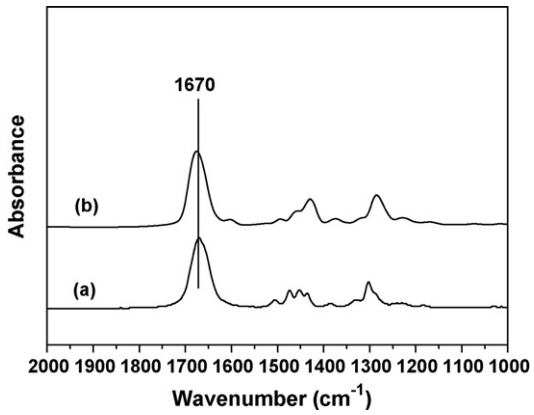

Fig. 5. FT-IR spectra of (a) neat PVP and (b) PVP/Au nanoparticle composite.

Table 2
Separation performance of PVP/Au composite membranes with varying weight ratios of PVP/Au nanoparticles

Weight ratio of PVP/Au	Total permeance (GPU)	Mixed gas selectivity (propylene/propane)
1/0	0.1	1.2
1/4.3	1.2	22

PVP, the peak representing the free carbonyl oxygen remained constant, indicating that the carbonyl oxygen were not coordinated to both the surface of nanoparticles and the stabilizer. Therefore, the polymer matrix, PVP, is regarded as an inert matrix for the gold nanoparticles, which is important for the use of gold nanoparticles in separation membranes.

3.3. Separation performance of PVP/Au nanocomposite membranes

The mixed gas separation performance of PVP/Au nanocomposite membranes have been evaluated and are provided in Table 2. Neat PVP membrane showed a mixed gas permeance of 0.1 GPU (1 GPU = 1×10^{-6} cm^3 (STP)/(cm^2 s cmHg)) and a selectivity for propylene/propane of 1.2. On the other hand, when the gold nanoparticles were incorporated into PVP, both the mixed gas permeance and the selectivity increased to 1.2 GPU and 22, respectively. This remarkable enhancement of the separation performance of the membranes is attributable to the olefin transport facilitated by the gold nanoparticles acting as effective carriers of olefins, which is possible due to the reversible interaction between the partially polarized gold nanoparticles and the olefin molecules.

4. Conclusions

In summary, novel facilitated olefin transport membranes consisting of PVP and gold nanoparticles were prepared for the separation of olefin/paraffin mixtures. Gold nanoparticles were prepared and stabilized by 4-dimethylaminopyridine; stabilization by DMAP was confirmed by XRD, TEM, and UV–vis spectroscopy. XPS and the measured zeta potential also verified the positively charged nature of the gold nanoparticles. As a result, PVP/Au nanocomposite membranes performed better than PVP membranes for separation of olefin mixtures, displaying an improved mixed gas permeance of 1.2 GPU and a selectivity of 22. Therefore, we conclude that the polarized gold nanoparticles can be used as an effective olefin carrier for facilitated olefin transport membranes.

Acknowledgements

This work was supported by Energy Technology R&D program (2006-E-ID11-P-13) under the Korea Ministry of Commerce, Industry and Energy (MOCIE). KC acknowledges the financial support of NSI-NCRC and the Ministry of Education through the Brain Korea 21 Program at Seoul National University. This work was also supported by ERC Program of KOSEF grant funded by the Korea government (MEST) (R11-2005-048-00000-0).

References

[1] S. Malynych, H. Robuck, G. Chumanov, Fabrication of two-dimensional assemblies of Ag nanoparticles and nanocavities in poly(dimethylsiloxane) resin, Nano Lett. 1 (2001) 647.
[2] P. Claus, H. Hofmeister, Electron microscopy and catalytic study of silver catalysts: structure sensitivity of the hydrogenation of crotonaldehyde, J. Phys. Chem. B 103 (1999) 2766.
[3] H. Tada, K. Teranishi, Y. Inubushi, S. Ito, Ag nanocluster loading effect on TiO_2 photocatalytic reduction of bis(2-dipyridyl)disulfide to 2-mercaptopyridine by H_2O, Langmuir 16 (2000) 3304.
[4] U. Nickel, A. zu Castell, K. Po¨ppl, S. Schneider, A silver colloid produced by reduction with hydrazine as support for highly sensitive surface-enhanced Raman spectroscopy, Langmuir 16 (2000) 9087.
[5] L. Quaroni, G. Chumanov, Preparation of polymer-coated functionalized silver nanoparticles, J. Am. Chem. Soc. 121 (1999) 10642.
[6] F. Peng, F. Pan, H. Sun, L. Lu, Z. Jiang, Novel nanocomposite pervaporation membranes composed of poly(vinyl alcohol) and chitosan-wrapped carbon nanotube, J. Membr. Sci. 300 (2007) 13.
[7] A.L. Ahmad, N.N.N. Mustafa, Sol–gel synthesized of nanocomposite palladium–alumina ceramic membrane for H_2 permeability: preparation and characterization, Int. J. Hydrogen Energy 32 (2007) 2010.
[8] S. Miachon, P. Ciavarella, L. van Dyk, I. Kumakiri, K. Fiaty, Y. Schuurman, J.-A. Dalmon, Nanocomposite MFI-alumina membranes via pore-plugging synthesis: specific transport and separation properties, J. Membr. Sci. 298 (2007) 71.
[9] E.N. Gribov, E.V. Parkhomchuk, I.M. Krivobokov, J.A. Darr, A.G. Okunev, Supercritical, CO_2 assisted synthesis of highly selective nafion–zeolite nanocomposite membranes for direct methanol fuel cells, J. Membr. Sci. 297 (2007) 1.
[10] H. Cong, M. Radosz, B.F. Towler, Y. Shen, Polymer–inorganic nanocomposite membranes for gas separation, Sep. Purif. Technol. 55 (2007) 281.
[11] M.L.D. Vona, Z. Ahmed, S. Bellitto, A. Lenci, E. Traversa, S. Licoccia, SPEEK-TiO_2 nanocomposite hybrid proton conductive membranes via in situ mixed sol–gel process, J. Membr. Sci. 296 (2007) 156.
[12] S.W. Chuang, S.L.C. Hsu, C.L. Hsu, Synthesis and properties of fluorine-containing polybenzimidazole/montmorillonite nanocomposite membranes for direct methanol fuel cell applications, J. Power Sources 168 (2007) 172.
[13] R. Guo, X. Ma, C. Hu, Z. Jiang, Novel PVA–silica nanocomposite membrane for pervaporative dehydration of ethylene glycol aqueous solution, Polymer 48 (2007) 2939.
[14] K. Friess, M. Šípek, V. Hynek, C. Panayiotou, Sorption of VOCs and water vapors in polylacetate membrane with nanocomposite filler, Desalination 200 (2006) 265.
[15] J. Qiu, K.-V. Peinemann, Novel organic nanocomposite membrane for pervaporation, Desalination 200 (2006) 435.
[16] S.W. Kang, J.H. Kim, K. Char, J. Won, Y.S. Kang, Nanocomposite silver polymer electrolytes as facilitated olefin transport membranes, J. Membr. Sci. 285 (2006) 102.
[17] M. Sairam, B.V.K. Naidu, S.K. Nataraj, B. Sreedhar, T.M. Aminabhavi, Poly(vinyl alcohol)–iron oxide nanocomposite membranes for pervaporation dehydration of isopropanol 1,4-dioxane and tetrahydrofuran, J. Membr. Sci. 283 (2006) 65.
[18] S. Takahashi, D.R. Paul, Gas permeation in poly(ether imide) nanocomposite membranes based on surface-treated silica. Part 1. Without chemical coupling to matrix, Polymer 47 (2006) 7519.
[19] M. Ollinger, H. Kim, T. Sutto, A. Piqué, Laser printing of nanocomposite solid-state electrolyte membranes for Li micro-batteries, Appl. Surf. Sci. 252 (2006) 8212.
[20] L. Lebrun, S. Bruzaud, Y. Grohens, D. Langevin, Elaboration and characterisation of PDMS–$HTiNbO_5$ nanocomposite membranes, Eur. Polym. J. 42 (2006) 1975.
[21] C.N.R. Rao, V. Vijayakrishnan, A.K. Santra, M.W.J. Prins, Dependence of the reactivity of Ag and Ni clusters deposited on solid substrates on the cluster size, Angew. Chem. Int. Ed. 31 (1992) 1062.
[22] Y.S. Kang, S.W. Kang, H. Kim, J.H. Kim, J. Won, C.K. Kim, K. Char, Interactions of the partially polarized surface of silver nanoparticles by *p*-benzoquinone with olefin and its implication to facilitated olefin transport, Adv. Mater. 19 (2007) 475.
[23] D.I. Gittins, F. Caruso, Spontaneous phase transfer of nanoparticulate metals from organic to aqueous media, Angew. Chem. Int. 40 (2001) 3001.
[24] S. Wang, S. Sato, K. Kimura, Preparation of hexagonal-close-packed colloidal crystals of hydrophilic monodisperse gold nanoparticles in bulk aqueous solution, Chem. Mater. 15 (2003) 2445.
[25] H. Tsunoyama, H. Sakurai, N. Ichikuni, Y. Negishi, T. Tsukuda, Colloidal gold nanoparticles as catalyst for carbon–carbon bond formation: application to aerobic homocoupling of phenylboronic acid in water, Langmuir 20 (2004) 11293.